ELSEVIER

Computers & Geosciences 32 (2006) 1512–1518

COMPUTERS & GEOSCIENCES

www.elsevier.com/locate/cageo

Short note

Incorporating nonlinear rules in a web-based interactive landform simulation model (WILSIM)

Wei Luo[a,*], Edit Peronja[b,1], Kirk Duffin[b], Jay A. Stravers[c]

[a]*Department of Geography, Northern Illinois University, DeKalb, IL 60115, USA*
[b]*Department of Computer Science, Northern Illinois University, DeKalb, IL 60115, USA*
[c]*Department of Geology and Environmental Geosciences, Northern Illinois University, DeKalb, IL 60115, USA*

Received 23 January 2005; received in revised form 7 December 2005; accepted 15 December 2005

1. Introduction

Many 3-D landform evolution computer models have been developed in recent years (Willgoose, 2005 and references therein). These models can be divided into two primary categories: physically based and rule-based. The physically based models (e.g., Ahnert, 1987; Willgoose et al., 1991; Howard, 1994; Tucker and Slingerland, 1994; Braun and Sambridge, 1997; Tucker et al., 2001) generally integrate local transport processes over the system scale and solve directly for the effects of water discharge by solving hydrodynamic equations, or by using contributing area as a proxy for discharge. Models in this category are generally complicated, time-consuming to run, and can be hard for students to grasp. The rule-based cellular automata models (e.g., Chase, 1992; Murray and Poala, 1994; Luo, 2001; Haff, 2001; Crave and Davy, 2001; Coulthard et al., 2002; Luo et al., 2004) can be advantageous, especially for educational purposes, because they are simple to implement but still maintain a close analogy between model structure and the physical systems being modeled.

The web-based interactive landform simulation model (WILSIM) is a rule-based model and has proved to be a useful tool in helping students visualize and understand the basic concepts and processes of landform evolution over geologic time (Luo et al., 2004; Luo et al., 2005). It adopts a simple cellular automata (CA) algorithm (Chase, 1992) and is implemented as a Java applet. At each time step (or iteration), a rainfall event (termed precipiton) is randomly dropped onto a cell of a topographic grid and routed to the lowest of its neighboring cells. The precipiton continues to flow downhill and, along the way, it erodes bedrock material and carries the sediment with it until it lands in a pit, reach the edges, or its carrying capacity is exceeded. This simple process is repeated (iterated) many times to simulate the first-order features of landform evolution. The Java applet implementation allows for the widest possible accessibility via a standard web browser and interactive user exploration of different scenarios, which is ideal for educational purposes (Luo et al., 2004). In the linear version of the model, the amount of erosion is simply proportional to local slope and erodibility at any given cell, and the precipitons (i.e., rainfall events) are independent of

*Corresponding author. Tel.: +1 815 753 6828; fax: +1 815 753 6872.
E-mail address: wluo@niu.edu (W. Luo).
[1]Now at DEVNET INC, 2254 Oakland Drive, Sycamore, IL 60178, USA.

0098-3004/$ - see front matter
doi:10.1016/j.cageo.2005.12.012

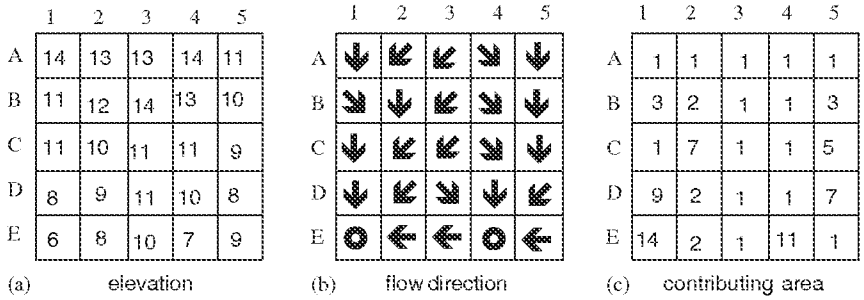

Fig. 1. A 5 × 5 grid illustrating how contributing area a is derived. (a) each number indicates elevation of that cell; (b) arrow indicates flow direction of each cell based on which neighboring cell is lowest; circle indicates a sink; (c) number indicates contributing area of each cell, i.e., number of cells flowing into a given cell. For example, cell C2 has B1, B2, and B3 flowing into it, so contributing area of cell C2 is equal to sum of contributing areas of B1 (3), B2 (2), and B3 (1), plus that of itself (1), so $a = 3 + 2 + 1 + 1 = 7$.

each other. Despite its simplicity, the linear version of WILSIM is capable of generating the first-order features of landform evolution. However, it does not explicitly simulate the nonlinear behavior of sediment erosion and transportation and precludes the simulation of interactions between storm events. This short note reports an improvement over these limitations by incorporating nonlinear rules into the model and compares the results with those from the linear version. For the basics of the CA algorithm and the details of the linear version of WILSIM, please refer to Luo et al. (2004) and Chase (1992). The nonlinear version of WILSIM can be accessed at the same URL as before: www.niu.edu/landform.

2. Nonlinear rules

2.1. The nonlinear rules

Unlike the linear version, where the amount of erosion is simply proportional to the slope and erodibility, in the nonlinear version of the model, the amount of erosion is calculated as follows:

$$P_e = e \times a^{n-1} \times s^m, \quad (1)$$

where P_e is the maximum possible erosion[2], e is the erodibility of material in the current cell, s is the local slope of the current cell, a is the contributing area to the current cell, and m and n are exponent coefficients.

This formulation is similar to Haff's (2001), however, the emphasis is different. Haff's model is focused on predicting the erosion and sedimentation pattern based on present day topography and in his model dropping precipitons (in his term waterbots) onto every cell and following them off the grid constitutes one iteration (Haff, 2001). The focus of WILSIM is to simulate the evolution of landform over geologic time, and one iteration consists of dropping one precipiton onto the grid and following it downhill until it stops or leaves the grid.

2.2. How to determine the contributing area a

The contributing area of a cell is defined here as the number of cells flowing into that cell. In the implementation, before each iteration of erosion and deposition of a precipiton starts, the program loops through the grids twice: the first time to determine the flow direction of each cell in the topographic grid by finding the lowest neighboring cell of each cell [i.e., follows the D8 algorithm (O'Callaghan and Mark, 1984; Jenson and Domingue, 1988)], and the second time to follow the flow direction and sum up the number of cells that flow into each cell [i.e., the contributing area a in Eq. (1)]. Fig. 1 schematically illustrates this process.

Once the flow direction and contributing area for each cell are determined, a precipiton, randomly dropped onto the grid, simply moves downhill continuously following the flow direction of the cell it is in and conducts erosion and deposition along the way as in the linear version except that the amount of erosion is now governed by Eq. (1). Before a new precipiton is dropped, the flow direction and contributing area need to be updated as the erosion and deposition from the current precipiton can change the elevation and thus change the flow direction and contributing area.

[2]The actual amount of erosion depends on the carrying capacity. The actual erosion cannot exceed the carrying capacity, which is proportional to discharge and slope (Chase, 1992).

Since the initial topographic grid in the model always starts with a slightly tilted plane and water flows downhill, the flow directions for cells higher than the target cell (i.e., the cell that the current precipiton first falls in) would not be changed by the current precipiton (region A in Fig. 2). Thus only flow directions for the cells lower than the target cell (region B in Fig. 2) will need to be updated for the next precipiton. Because we can not predetermine where the new precipiton will go in region B, every cell in region B will be updated. Compared with updating the entire grid, this approach nonetheless reduces the number of calculations considerably and speeds up the simulation processing time.

By incorporating the contributing area into the calculation of erosion, the precipitons are no longer independent, because the erosion of previous precipitons would increase the contributing area (especially for cells in the valleys), which will in turn have a direct and explicit impact on the erosion of the current and future precipitons according to Eq. (1). Since contributing area can be considered a proxy of discharge, the erosion is, in essence, nonlinearly related to a long-term average of the discharge (averaged over many iterations). This is in fact what happens in the real world in valley development and subsequent incision.

When $m = n = 1$ in Eq. (1), $P_e = c \times e \times s$, (i.e., the amount of erosion is directly proportional to slope and erodibility), it becomes the linear case. The new model thus incorporates both the linear and nonlinear components. The previous linear version of the model is faster since it simply deals with a 3×3 local neighborhood and does not require the two additional loops before each iteration to determine flow direction and contributing area. However, the nonlinear model more effectively reproduces the natural evolution of fluvial landscapes including increased resolution for specific patterns of erosion and deposition.

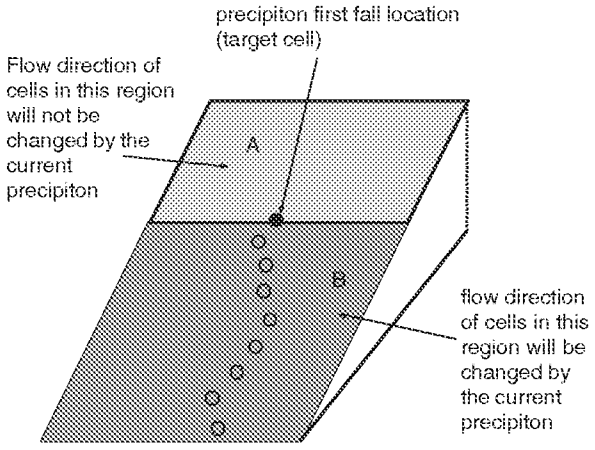

Fig. 2. Schematic diagram showing which part of topographic grid (cells) needs to be updated for flow direction after an iteration of erosion and deposition is completed before a new iteration starts. Only cells lower than target cell needs to be updated.

3. What's new in the graphical user interface (GUI)?

3.1. The exponent coefficients m and n

The nonlinear exponents m and n are located under the OPTIONS tab, Erodibility subtab (Fig. 3). The default values for m and n are 1.2, but they may be changed by clicking on the button next to *n value* or *m value* and dragging the slider to the right as shown in Fig. 3.

3.2. Fractal dimension

To show the changes in roughness of the topographic surface as it evolves over time, we added the FRACTAL tab to display a graph of fractal dimension. Simply speaking, fractal dimension is a number used to measure the roughness or complexity of an object (Chase, 1992), and the roughness or complexity remains more or less the same (self-similar) at different magnification scales (e.g., a shoreline will have similar complexity at varying magnification scales). For a line, the fractal dimension ranges between 1 (a perfectly smooth line) and 2 (a line that is so jagged that it fills the 2-D plane). For a surface, the fractal dimension

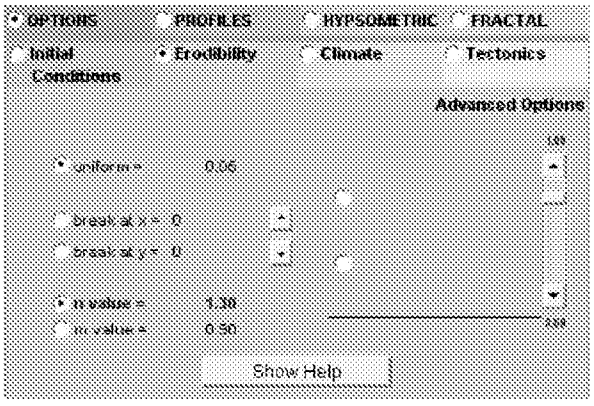

Fig. 3. Diagram showing where nonlinear parameters n and m can be changed in GUI.

ranges between 2 (a relatively smooth surface) and 3 (a space-filling surface). In general, the larger the fractal dimension value, the rougher the surface. The fractal dimension presented here is computed using the cubic covering method discussed in Voss (1986) and Zhou and Xie (2003). It is displayed at every 10% increment of the total iterations (see Figs. 4(c) and (d)).

4. Comparison of results: linear vs. nonlinear model

Here, we present the results from an example scenario with the following parameters: constant erodibility, constant climate, and varied tectonic uplift. That is, the erodibility of the surface was uniform across the grid, the rainfall rate remained constant throughout the simulation duration, and the top 60% of the topographic grid (row 40 and above) was being uplifted. Results from both the linear and nonlinear versions were shown in 3-D snapshots, 2-D profiles, hypsometric curves, and fractal dimension plots to demonstrate the improvement of the nonlinear model (Fig. 4).

Both versions produced the escarpment created from tectonic uplift, with the alluvial fans emanating from the escarpment, and the drainage networks developed in the plateau through headward erosion. However, the headward erosion in the nonlinear model extended further upstream as compared with that in the linear model. It also formed a more integrated drainage network (higher link frequency) on the uplifted plateau and larger alluvial fans at the base of the escarpment (Figs. 4(a) and (b)). This is because in the nonlinear model the precipitons are inter-related and the erosion is nonlinearly related to a long-term average of the discharge (averaged over many iterations). Thus, the erosion in the nonlinear model is more effective in reproducing natural forms of fluvial incision in which steeper slopes created by erosion further promote capturing and development of a larger and more integrated drainage area.

The larger erosional power in the nonlinear model is also shown in the row profiles at row 45 (5 rows upslope from the uplifting escarpment at row 40) (Fig. 4(c) and (d)). In the linear model, as the uplift progressed, vertical incision into bedrock rarely cut down below its initial bedrock elevation (at around 21 elevation units). However, the bedrock erosion in the nonlinear model cut down 2 units below its original bedrock elevation, forming steeper V-shaped valleys. On the other hand, sediments also accumulated on the lower valley floors in the nonlinear model, contrary to earlier expectations (Luo et al., 2004). The maximum sediment thickness in the valleys for the nonlinear model (~6 elevation units) is larger than that for the linear version (~5 elevation units), probably because of the large amount of sediments eroded from the uplands (due to a much larger catchment area in the nonlinear model) that are transported and deposited here.

The hypsometric curves shown here are based on the entire topographic grid, not on a specific watershed like traditional hypsometric curves. However, they can still effectively portray the relative amount of erosion of the entire grid. The curves clearly show more headward extension and escarpment retreat in the nonlinear model. Hypsometric curve results also revealed one of the limitation of relative hypsometry, i.e., it is sensitive to local peaks (higher elevation plateau remnants). The local peaks created by continued tectonic uplift throughout the simulation actually forced the lower part of the curve to move downward (relatively) through time, making it appear to have more erosion in the lower part of the landform (the nonuplifting stable part of the landform).

The fractal dimension plot (Fig. 4(c)) shows that the nonlinear model is rougher (higher fractal dimension value) than its linear counterpart at the same simulation interval. This is again consistent with expectations and results from snapshots, profiles, and hypsometric curves. Sensitivity tests show that the higher the value of n, the rougher the resulting landform; the higher the value of m, the smoother the resulting landform. This is because the contributing area a is an integer greater than or equal to 1, and the slope s is often less than 1 (the difference between the current cell and its lowest neighbor divided by the cell size).

5. Summary

The nonlinear version of WILSIM integrates the simplicity of a CA algorithm and the complexity of nonlinear processes for sediment erosion, transport, and deposition to simulate landform evolution more realistically. Incorporating nonlinear rules into the CA-based Java applet brings the model closer to reality (observed natural landforms) while maintaining its easy accessibility and interactiveness for educational purposes. In the nonlinear version, the amount of erosion at any given cell is a power

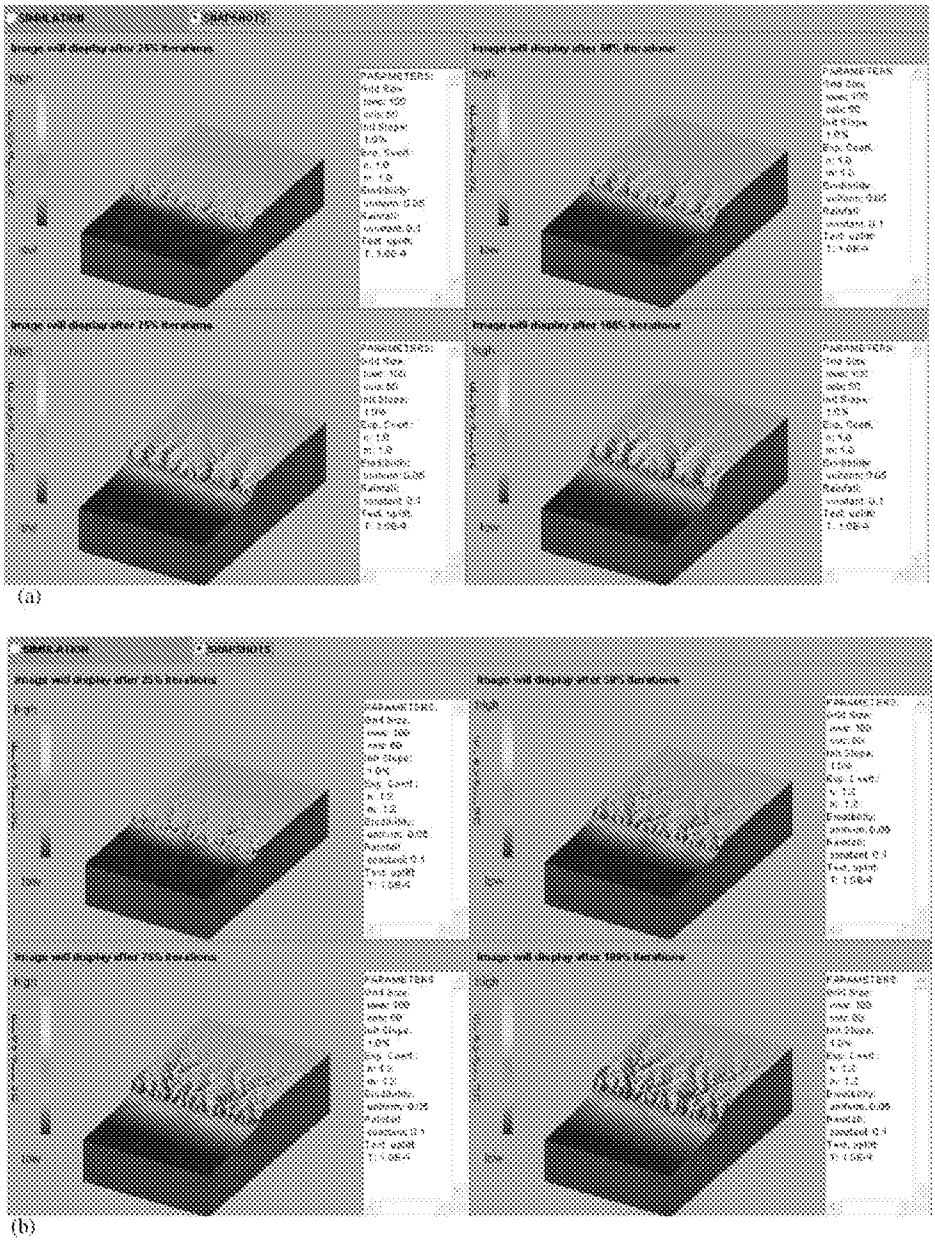

Fig. 4. (a) Snapshots of linear version results for a scenario of constant climate, uniform erodibility and tectonic uplift at row 40; (b) Snapshots of nonlinear version results for same scenariol; (c) row profile at row 45, hypsometric curve and fractal dimension plot of linear version results as it evolves over time; (d) row profile at row 45, hypsometric curve and fractal dimension plot for nonlinear version results.

function of slope and discharge, which is related to the contributing area (represented by the number of cells flowing into the cell under consideration, i.e., precipitons are no longer independent but interrelated). This new model represents two major improvements over the previous linear version, i.e., (1) it explicitly simulates the nonlinear processes of surficial erosion, sediment transport, and sediment deposition in the natural world and (2) the precipitons are interdependent through the contributing area. Compared with the linear model, the nonlinear version generally creates a rougher landscape, more integrated drainage network, and steeper valley slopes.

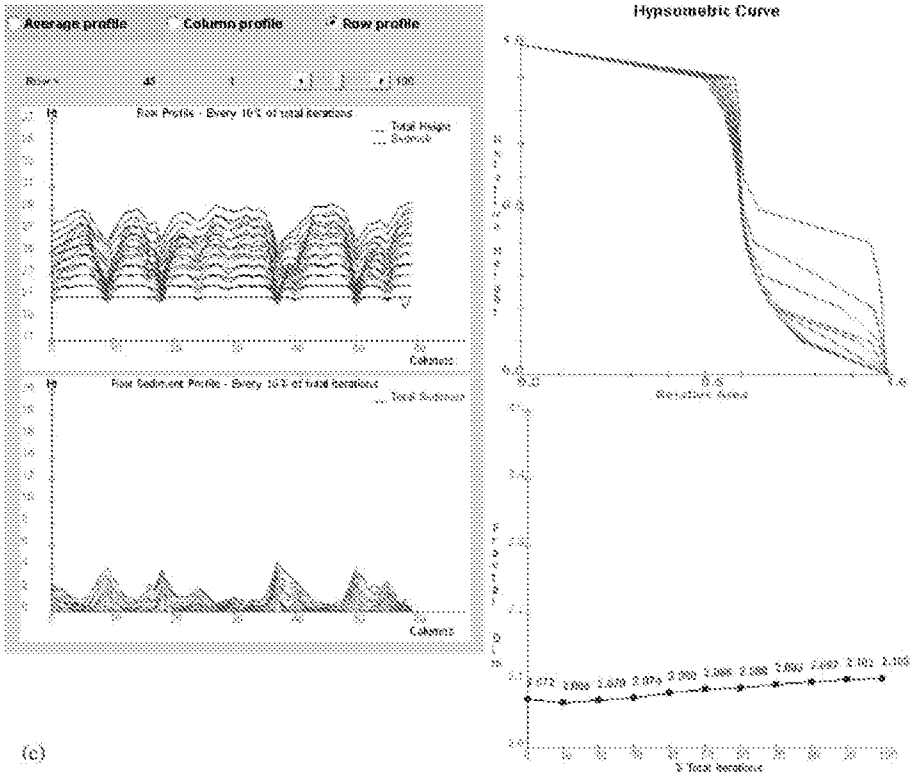

(c)

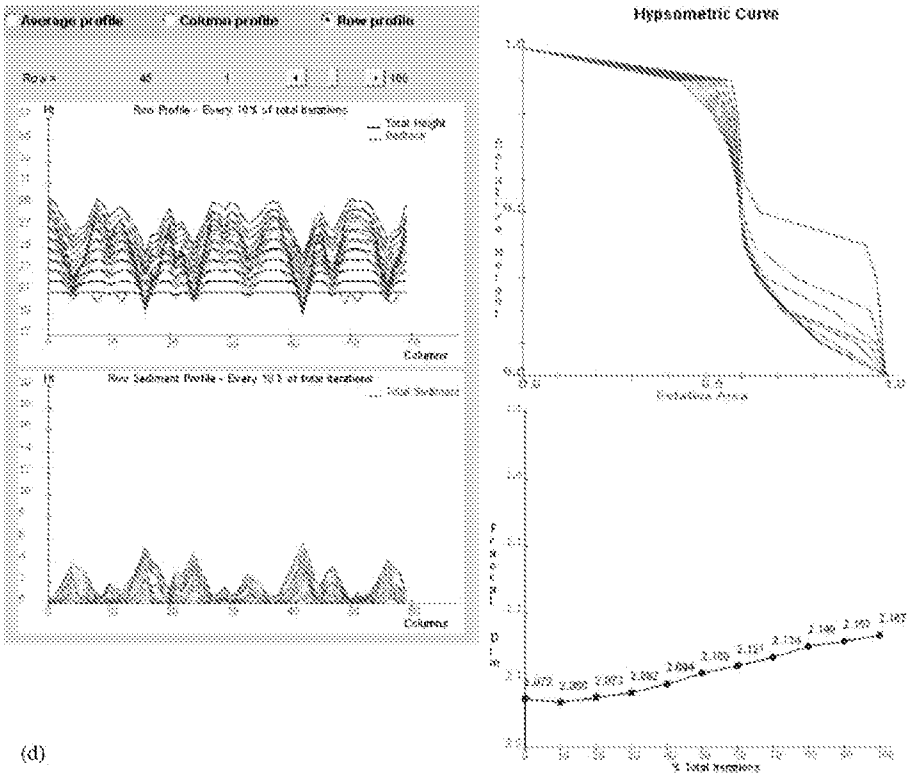

(d)

Fig. 4. (*Continued*)

Acknowledgements

This project is funded by National Science Foundation (NSF) Course Curriculum and Laboratory Improvement (CCLI) Program (Award no. DUE-0127424). We thank Information Technology Services (ITS) at Northern Illinois University for hosting the website and Harry Clark for technical assistance.

References

Ahnert, F., 1987. Approaches to dynamic equilibrium in theoretical simulations of slope development. Earth Surface Processes and Landforms 12, 3–15.

Braun, J., Sambridge, M., 1997. Modeling landscape evolution on geologic time scales: a new method based on irregular spatial discretization. Basin Research 9 (1), 27–52.

Chase, C.G., 1992. Fluvial landsculpting and the fractal dimension of topography. Geomorphology 5, 39–57.

Coulthard, T., Macklin, M.G., Kirkby, M.J., 2002. A cellular model of Holocene upland river basin and alluvial fan evolution. Earth Surface Processes and Landforms 27 (3), 269–288.

Crave, A., Davy, P., 2001. A stochastic "precipiton" model for simulation erosion/sedimentation dynamics. Computers & Geosciences 27, 815–827.

Haff, P.K., 2001. Waterbots. In: Harmon, R.S., Doe, W.W.III. (Eds.), Landscape Erosion and Evolution Modeling. Kluwer Academic/Plenum Publishers, New York, NY, pp. 239–275.

Howard, A.D., 1994. A detachment-limited model of drainage basin evolution. Water Resources Research 30, 2261–2285.

Jenson, S.K., Domingue, J.O., 1988. Extracting topographic structure from digital elevation data for geographic information system analysis. Photogrammetric Engineering and Remote Sensing 54 (11), 1593–1600.

Luo, W., 2001. LANDSAP: a coupled surface and subsurface cellular automata model for landform simulation. Computers and Geosciences 27 (3), 363–367.

Luo, W., Duffin, K.L., Peronja, E., Stravers, J.A., Henry, G.M., 2004. A web-based interactive landform simulation model (WILSIM). Computers & Geosciences 30 (3), 215–220.

Luo, W., Stravers, J.A., Duffin, K.L., 2005. Lessons learned from using a web-based interactive landform simulation model (WILSIM) in a general education physical geography course. Journal of Geoscience Education 53 (5), 489–493.

Murray, A.B., Poala, C., 1994. A cellular model of braided rivers. Nature 371, 54–57.

O'Callaghan, J.F., Mark, D.M., 1984. The extraction of drainage networks from digital elevation data. Computer Vision, Graphics, and Image Processing 28 (3), 323–344.

Tucker, G.E., Slingerland, R., 1994. Erosional dynamics, flexural isostasy, and long-lived escarpments: a numerical modeling study. Journal of Geophysical Research-Solid Earth 99 (B6), 12229–12243.

Tucker, G.E., Lancaster, S.T., Gasparini, N.M., Bras, R.L., Rybarczyk, S.M., 2001. An object oriented framework for distributed hydrologic and geomorphic modeling using triangulated irregular networks. Computers & Geosciences 27, 959–973.

Voss, R.F., 1986. Random fractals: characterization and measurement. Physica Scripta T13, 27–32.

Willgoose, G., Bras, R.L., Rodriguez-Iturbe, I., 1991. A coupled channel network growth and hillslope evolution model, 1. Theory. Water Resources Research 27, 1671–1684.

Willgoose, G., 2005. Mathematical modeling of whole landscape evolution. Annual Review of Earth Planetary Science 33, 443–459.

Zhou, H.W., Xie, H., 2003. Direct estimation of the fractal dimensions of a fracture surface of rock. Surface Review and Letters 10 (5), 751–762.